Inhibiting Aggregation of α-Synuclein with Human Single Chain Antibody Fragments

ARTICLE *in* BIOCHEMISTRY · APRIL 2004

Impact Factor: 3.02 · DOI: 10.1021/bi036281f · Source: PubMed

Inhibiting Aggregation of α-Synuclein with Human Single Chain Antibody Fragments†

Sharareh Emadi,[#] Ruitian Liu,[#] Bin Yuan,[#] Philip Schulz,[#] Chad McAllister,[‡] Yuri Lyubchenko,[‡] Anne Messer,[§] and Michael R. Sierks*,[#]

Department of Chemical and Materials Engineering, Department of Microbiology, Arizona State University, Tempe, Arizona 85287, and Wadsworth Center, New York State Department of Health and Department of Biomedical Sciences, University at Albany, Albany, New York 12201

Received December 18, 2003; Revised Manuscript Received January 14, 2004

ABSTRACT: The α-synuclein protein has been strongly correlated with Parkinson's disease (PD) and is a major component of the hallmark Lewy body aggregates associated with PD. Two different mutations in the α-synuclein gene as well as increased gene dosage of wild-type α-synuclein all associate with early onset cases of PD; and transgenic animal models overexpressing α-synuclein develop PD symptoms. α-Synuclein, a natively unfolded protein, can adopt a number of different folded conformations including a *β*-sheet form that facilitates formation of numerous aggregated morphologies, including long fibrils, spherical and linear protofibrils, and smaller aggregates or oligomers. The roles of the various morphologies of α-synuclein in the progression of PD are not known, and different species have been shown to be toxic. Here we show that single chain antibody fragments (scFv's) isolated from naïve phage display antibody libraries can be used to control the aggregation of α-synuclein. We isolated an scFv with nanomolar affinity for monomeric α-synuclein ($K_D = 2.5 \times 10^{-8}$ M). When co-incubated with monomeric α-synuclein, the scFv decreased not only the rate of aggregation of α-synuclein, but also inhibited the formation of oligomeric and protofibrillar structures. The scFv binds the carboxyl terminal region of α-synuclein, suggesting that perturbation of this region can influence folding and aggregation of α-synuclein in vitro along with the previously identified hydrophobic core region of α-synuclein (residues 61−95, particularly residues 71−82). Since the scFv has been isolated from an antibody library based on human gene sequences, such scFv's can have potential therapeutic value in controlling aggregation of α-synuclein in vivo when expressed intracellularly as intrabodies in dopaminergic neurons.

Parkinson's disease (PD)[1] is characterized by progressive loss of dopaminergic neurons in the substantia nigra and formation of fibrillar cytoplasmic inclusions (Lewy bodies) (*1*). α-Synuclein has been identified as a major component of the Lewy bodies and Lewy neurites (*2*−*4*) found in PD and other neurodegenerative disorders, including the Lewy body variant of Alzheimer's disease, dementia with Lewy bodies, as well as the glial and neuronal cytoplasmic inclusions of multiple system atrophy (*5*−*9*). In a small number of PD cases, a genetic correlation was found in families having either of two different point mutations in a presynaptic protein, α-synuclein, (A53T and A30P) (*10*, *11*), and increased gene dosage of wild-type α-synuclein was also correlated with PD (*12*). Furthermore, expression of wild-type and mutant human α-synuclein respectively in transgenic mice and flies leads to motor disorder and neuronal inclusions similar to PD (*13*−*15*). Therefore, α-synuclein has become a primary target for understanding and controlling the progression of PD.

The N-terminal region of α-synuclein (residues 1−95) contains seven imperfect repeats of 11 amino acids, six of which contain the six-residue core consensus sequence KTK-(E/Q)GV. This repeat section is similar to that found in the amphipathic α-helical region of the lipid-binding domain of apolipoproteins. α-Synuclein was shown to bind acidic but not neutral phospholipids, where binding also resulted in stabilization of α-helical content (around 80%) in the synuclein structure (*16*).

A 12-residue hydrophobic region (residues 71−82, VT-GVTAVAQKTV) has been shown to be essential for aggregation of α-synuclein in vitro (*17*). The C-terminal region of α-synuclein (residues 96−140) is much more hydrophilic and is enriched with acidic glutamate and aspartate residues. While α-synuclein normally exists in an unfolded conformation, it can adopt several different folded conformations depending on the environment, including small aggregates, oligomers, protofibrils, and the fibrillar structures found in Lewy bodies (*18*−*22*). Temperature, pH, and metal ions all play a role in the in vitro conversion of

† This work was supported in part by grants from the NIH (AG17984) and the Arizona Disease Control Research Commission.

* Corresponding author: Michael R. Sierks, Chemical and Materials Engineering, Box 876006, Tempe, AZ 85287-6006; phone: 480-965-2828; fax: 480-965-0037; e-mail: sierks@asu.edu.

[#] Department of Chemical and Materials Engineering, Arizona State University.

[‡] Department of Microbiology, Arizona State University.

[§] University at Albany.

[1] Abbreviations: PD, Parkinson's disease; α-syn, α-synuclein; scFv, single chain antibody fragment; AFM, atomic force microscope; NAC, nonamyloid component; A30P, human A30P α-synuclein; A53T, human A53T α-synuclein; ThT, thioflavin T.

10.1021/bi036281f CCC: $27.50
Published on Web 02/20/2004

α-synuclein into β-sheet conformation (*23*−*25*). While misfolding and aggregation of α-synuclein is required for Lewy body formation and is a pathological feature of PD, the role of α-synuclein misfolding in PD is still unclear. However, α-synuclein aggregation is likely to be important in the etiology of PD since mutant forms of α-synuclein linked to familial PD promote aggregation of α-synuclein in vitro (*19*, *21*, *26*−*28*), and overexpression of α-synuclein in neuronal cell lines (*29*), transgenic mice (*14*, *15*), and drosophila (*13*) leads to formation of intracellular Lewy-body like inclusions and other PD-like symptoms.

Since aggregation of α-synuclein is associated with several neurodegenerative diseases, developing compounds that can control α-synuclein folding and aggregate formation may have therapeutic applications for controlling the progression of PD and other related diseases. Here we show that a recombinant human single chain variable domain antibody fragment (scFv) isolated from a naïve phage display antibody library by panning against monomeric α-synuclein binds α-synuclein with relatively high affinity ($K_D = 2.5 \times 10^{-8}$ M) and inhibits in vitro aggregation. Such antibody constructs have potential therapeutic applications since they are based on human gene sequences and can be expressed intracellularly, but are not isolated by immunization and do not contain the constant domain region responsible for initiating complement response (*30*). This approach has been used successfully to counteract effects of misfolded mutant huntingtin protein, providing precedent for the use of intrabodies in neurodegenerative disease (*31*−*33*).

EXPERIMENTAL PROCEDURES

Materials. The Griffin 1 phage library was obtained from the Medical Research Council (Cambridge, England) (*34*). Samples of wild-type human recombinant monomeric and fibrillar α-synuclein were a generous gift of Dr. Peter Lansbury (Harvard Medical School). All chemicals were obtained from Sigma-Aldrich (St. Louis, MO) unless otherwise indicated.

Biopanning. The phage library (*34*) was propagated essentially as described in the Medical Research Council protocols (www.mrc.cpe.cam.ac.uk). Selection of phage was performed using five rounds of biopanning essentially as described (*35*). Briefly, Immunotubes (Maxisorb, Nunc) were coated overnight at 4 °C with 10 μg/mL recombinant human monomeric α-syuclein in 50 mM carbonate-bicarbonate, pH 9.6. To decrease nonspecific binding, we added 3% BSA in PBS (10 mM phosphate, 150 mM NaCl, pH 7.4) for 2 h at 37 °C. Around 10^{12} phage titer units in 4 mL of 1% BSA-PBS were added to the immunotube and incubated for 30 min under continuous rocking, followed by 90 min without rocking at 22 °C. Bound phage were eluted in 1 mL of triethylamine (7.18 M), and neutralized with 0.5 mL of 1 M Tris/HCl, pH 7.4. To determine the number of eluted phage, infected *Escherichia coli* cells were plated in serial dilution on agar containing ampicillin (100 μg/mL) plates. Eluted phage were amplified by infection of fresh *E. coli* TG1 cells in the presence of helper phage VCSM13 (Stratagene, Cedar Creek, TX) as described previously (*35*). The phage were purified from the culture supernatant by poly(ethylene glycol) precipitation (poly(ethylene glycol) 6000/NaCl, Merck, Darmstadt, Germany) and resuspended in PBS.

Selection by Phage ELISA. (a) Polyclonal ELISA. High binding polystyrene microtiter plates (Corning, USA) were coated with human recombinant monomeric α-synuclein (10−100 μg/mL) essentially as described above for coating immunotubes. Nonspecific binding was blocked by incubation with 3% BSA for 2 h at 37 °C. Around 10^{10} titer units of PEG precipitated phage in 100 μL of 2% BSA-PBS were added to the wells and incubated for 90 min at room temperature. Bound phage were detected after a 1 h incubation with a 1:5000 dilution of anti-M13 antibody horseradish peroxidase (HRP) conjugate (Amersham Biosciences, Piscataway, NJ). A total of 100 μL of the HRP substrate 3,3′,5,5′-tetramethylbenzidine (TMB) was added and the reaction was stopped after 20 min with 2 M H_2SO_4 (VWR, West Chester, PA). Activity was determined by subtracting OD_{650} from OD_{450} using a Wallac 1420 plate reader (PerkinElmer, Shelton, CT).

(b) Monoclonal ELISA. 96 individual clones were grown essentially as described (www.mrc.cpe.cam.ac.uk). The high binding microtiter plates were coated with 1 μg/mL of monomeric α-synuclein and blocked as described above. Bacterial supernatant containing antibody fragments was diluted with an equal volume of blocking buffer and added to each well (100 μL/well). Bound phage was detected as described above.

Soluble scFv ELISA. Soluble scFv was produced by expressing recovered phagemid samples in the nonsuppresor *E. coli* strain HB2151 (*36*). Individually selected clones were grown essentially as described (www.mrc.cpe.cam.ac.uk) and scFv production induced by addition of 1 mM isopropyl-β-D-thiogalactopyranoside (IPTG) and incubated overnight at 30 °C. Supernatant samples were separated by centrifugation (1500*g*, 30 min, 4°C) and periplasmic fractions were prepared as described (*37*). Both supernatant and periplasmic fractions were assayed for antigen binding by ELISA as described above. High affinity microtiter plates were coated with 1 μg/mL of human recombinant monomeric α-synuclein. Bound antibodies were detected after a 1-h incubation using a 1/500 dilution of anti-c-Myc tag (9E10) mouse monoclonal antibody HRP-conjugate (Santa Cruz Biotechnology, Santa Cruz, CA).

Production and Purification of scFv. Soluble scFv from selected clones was produced as described above. The supernatant and periplasmic fractions from a 1-L culture were combined, passed through a 0.2 μM filter (Whatman, Clifton, NJ), and concentrated in a tangential flow filter (Millipore) using a 10 kDa cutoff membrane (Millipore, Billerica, MA). Concentrated samples were dialyzed overnight against 0.5 M NaCl−PBS and then purified by immobilized metal ion affinity chromatography (*38*) using a HiTrap Chelating HP column (Amersham Biosciences) charged with $NiSO_4$. The fractions were eluted with 10−25 mM imidazole and dialyzed overnight into PBS. The eluates were analyzed by SDS−PAGE on 15% polyacrylamide gels (Bio-Rad, Hercules, CA).

PCR Amplification. Since clones isolated from phage libraries prepared in a manner similar to the Griffin 1 library may frequently contain deletions (*39*), we tested for presence of the full-length 750 base pair scFv insert by PCR (polymerase chain reaction) after 21 cycles of amplification using the phagmid DNA as template and the backward primer, LMB3 (5′-CAGGAAACAGCTATGAC), and for-

ward primer, fdSeq1 (5′-GAATTTTCTGTATGAGG) as described (*40*). PCR analysis was performed using 1.5% (w/v) agarose gels (Merck).

Restriction Endonuclease Digestion. Plasmid was isolated from TG1 cells producing the scFv using Qiagen Plasmid Miniprep kit (QIAGEN, Valencia, CA) according to the manufacturer's protocols. The presence of the scFv gene was confirmed by incubating 40 μL of plasmid in a 100 μL digestion mixture containing 100 mM NaCl, 50 mM Tris-HCl (pH 7.9), 10 mM $MgCl_2$, 1 mM dithiothreitol, and 20 U each of the restriction enzymes, *NcoI* and *NotI*. The mixture was incubated for 6 h at 37 °C. The restriction enzyme digestion products were analyzed using a 1% agarose gel.

Binding Kinetics. Affinity measurements were performed using a BIAcore X biosensor (BIAcore Inc., Piscataway, NJ). A CM5 sensor chip (BIAcore) was activated as recommended by the manufacturer using an equimolar mix of NHS (*N*-hydroxysuccinimide) and EDC (*N*-ethyl-*N*′-(dimethylaminopropyl)carbodiimide), and coupled with 20 μg/mL of human recombinant monomeric α-synuclein in pH 4.0 sodium acetate buffer, and then blocked with ethanolamine. The final coupling level of monomeric α-synuclein was 180 RU. The association and dissociation rate constants (k_a and k_d) were determined using an scFv concentration range of 166.25−997.5 nM with HBS-EP (0.01 M HEPES, 0.15 M NaCl, 3 mM EDTA, 0.005% (v/v) surfactant P20, pH 7) (BIAcore) as a running buffer at a flow rate of 30 μL/min. The sensor surface was regenerated using 100 mM NaOH. Kinetic parameters were evaluated using BIAevaluation 3.1 software (BIAcore). Data were obtained by subtracting the readings obtained from the control cell without immobilized α-synuclein from the readings obtained in the sample cell containing α-synuclein.

Thioflavin T Aggregation Assay. α-Synuclein was dissolved at final concentration of 40 μM in 10 mM phosphate buffer (PB) pH 7, filtered through a 0.2 μM filter, and incubated at 37 °C either with or without the addition of 40 μM scFv. Aggregation of α-synuclein was measured in triplicate at various time points by adding 30 μL aliquots of the above solution into 2 mL of 5 μM thioflavin T solution in 50 mM phosphate buffer, pH 6.5. Fluorescence intensity of the samples were measured at an excitation wavelength of 450 nm and an emission wavelength of 482 nm on a Shimadzu RF-551 spectrofluorophotometer using 1-cm light-path quartz cuvettes with both excitation and emission bandwidth of 5 nm.

Atomic Force Microscope (AFM) Imaging. 1-(3-Aminopropyl)silatrane (APS)-modified mica was used as an AFM substrate (*41*, *42*). Five microliters of sample was placed on APS-mica for 2 min, rinsed with deionized water, and dried with argon as described earlier (*41*, *42*). Images were acquired in air using a MultiMode SPM NanoScope III system (Veeco/Digital Instruments, Santa Barbara, CA) operating in Tapping Mode using silicon probes (Olympus). To determine filament widths, either circular plasmid DNA was co-deposited onto samples, or circular plasmid DNA samples were imaged using a single tip immediately before and after imaging of protofibril samples. DNA is a convenient standard (2-nm-wide filaments) to determine the filament diameter of other samples from AFM data. Width measurements were ascertained from the AFM images using Femtoscan software (Advanced Technologies Center, Moscow, Russia). The diameters of fibrils were retrieved from the AFM width data (*W*) using a simplified expression for W and the filaments radii (R_1 and R_2, respectively) $W^2 = 16R_1R_2$. This expression was a simplified version of the expression obtained in ref *43* assuming a spherical shape of the AFM tip. Nanoscope software version 5.12 was used to determine the rms values of the images.

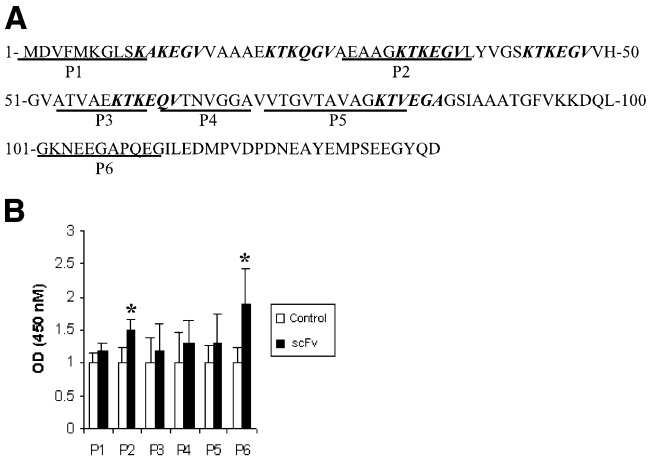

FIGURE 1: (A) Amino acid sequence of α-synuclein. The sequence of α-synuclein is shown with the repeat sections highlighted in bold and italic font. The six peptide fragments studied are underlined. P1: MDVFMKGLSK (residues 1−10, N-terminal domain), P2: AEAAGKTKEGV (residues 27−37, N-terminal domain), P3: ATVAEKTK (residues 53−60, N-terminal domain), P4: QVTNVGGA (residues 62−69, NAC domain), P5: VVTGVTAVAGKT (residues 70−81, NAC domain), P6: GKNEEGAPQEG (residues 101−111, C-terminal domain). NAC represents the nonamyloid component of α-synuclein that was identified in Alzheimer's plaques. (B) Epitope mapping. The six peptides, P1, P2, P3, P4, P5, and P6, were immobilized on sulfhdryl binding microtiter plates. After blocking, the plate was incubated for 2 h at room temperature with 40 μg/well of purified scFv. Bound scFv was detected by an anti-c-Myc tag (9E10) HRP conjugate. Activity was measured by comparing absorbance at 450 nm between a control well (without immobilized peptide) to the sample well (with peptide) where the control value was normalized to 1. Data represent the average ± standard deviation (STDV) of four separate experiments. A *p* value ($*p < 0.05$) was considered to be statistically significant (paired student t-test).

Peptide Synthesis. Six different peptides spanning different regions from residues 1 to 111 of human α-synuclein (*17*) were synthesized at the Protein Chemistry Core Facility at Arizona State University (Figure 1A). Peptides were synthesized on a Milligen Biosearch 9050 peptide synthesizer using Fmoc chemistry. All peptides were synthesized with an additional cysteine residue at the amino-terminal end to allow for specific immobilization to sulfhydryl binding microtiter plate well surfaces through thiol coupling.

Epitope Mapping. Sulfhydryl binding microtiter plates (Corning, USA) were coated overnight with 5 μg of each peptide in 100 μL of PBS containing 1 mM EDTA (pH 6.4). After washing and blocking with 2% nonfat milk in PBS (MPBS) for 2 h at room temperature, the plates were incubated with 100 μg/mL of purified scFv or 200 μL of a crude periplasmic fraction (*37*) in 1% MPBS for 2 h at room temperature. Bound antibody was detected using anti-c-Myc tag (9E10) mouse monoclonal antibody HRP-conjugate as described for soluble scFv ELISA. Activity was measured by comparing absorbance at 450 nM of a control well

(without immobilized peptide) to the sample well (with peptide) and normalizing the control values to 1. Data represent the average of four separate experiments. *P* values < 0.05 were considered to be statistically significant using a paired student t-test.

RESULTS

Biopanning against Human Monomeric α-Synuclein. Phage titers of the eluted fractions obtained after each round of panning against monomeric α-synuclein increased steadily from 10^4 after the first round to around 10^8 after the fifth round, indicating successful enrichment of the library. In addition, polyclonal phage ELISA, using aliquots of eluted phage from the second through fifth round also indicated an increase in phage binding after each round (data not shown). The pool of phage eluted from the fifth round of panning was used to infect *E. coli* TG1. We tested 96 individual clones and selected the 10 strongest binding scFv's as indicated by ELISA for DNA analysis. Restriction endonuclease digestion analysis of phagemid DNA samples indicated six clones either contained large deletions or were completely missing the scFv insert. On the basis of the ELISA and restriction digest results, we selected the strongest binding full-length scFv for further study.

Expression and Purification of Soluble scFv. For production of soluble scFv, *E. coli* HB2151 cells were infected with the phagemid DNA. HB2151 recognizes the amber stop codon at the junction between the scFv gene and phage minor coat-protein pIII. The scFv gene contains both a c-myc-tag and $(His)_6$-tag sequence at the C-terminus, facilitating detection of the scFv with anti-c-myc tag antibody and rapid purification by immobilized metal affinity chromatography, respectively (www.mrc.cpe.cam.ac.uk).

Purified scFv was obtained by using 1-L shake flask cultures, concentrating the combined periplasmic and supernatant fractions, and then purifying the scFv by immobilized metal affinity chromatography. Analysis of eluted fractions by SDS−PAGE revealed the presence of a single protein band having a molecular mass of around 29 kDa (Figure 2A).

Binding Kinetics of scFv to Human Monomeric α-Synuclein. The binding affinities of the purified scFv isolated against monomeric α-synuclein was determined by surface plasmon resonance. Recombinant human monomeric α-synuclein was coupled to the sensor chip and the association and dissociation curves at six different scFv concentrations were determined (Figure 2B). By fitting the association and dissociation curves to a single binding site model, we calculated an association rate constant of $k_a = 3.02 \times 10^4$ M^{-1} s^{-1}, and a dissociation rate constant of $k_d = 7.5 \times 10^{-4}$ s^{-1} (Figure 2B). The resulting dissociation equilibrium constant, $K_D = k_a/k_d = 2.48 \times 10^{-8}$ M, indicates relatively high affinity of the scFv for monomeric α-synuclein.

Epitope Mapping. To identify which epitopes of α-synuclein the scFv binds to, we synthesized a series of six synthetic peptides spanning residues 1−111 of human α-synuclein (Figure 1A) and used these for epitope mapping. As determined by ELISA, the scFv showed statistically significant affinity ($P < 0.05$) for peptide 2 (AEAAGKTKEGV) and 6 (GKNEEGAPQEG) corresponding to residues 27−37 and 110−111 of α-synuclein, respectively (Figure 1B).

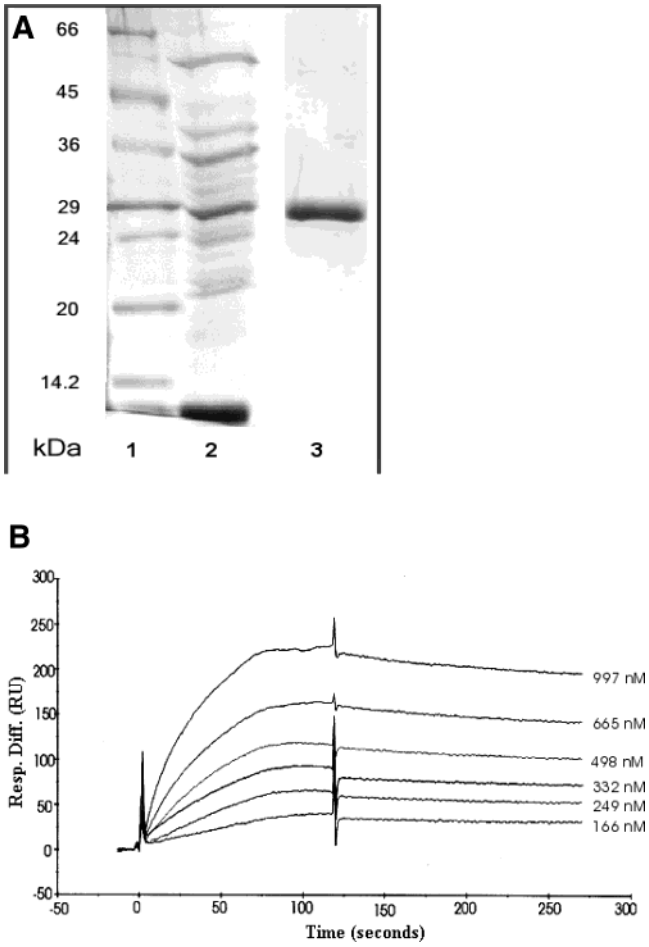

FIGURE 2: (A) SDS−PAGE analysis of recombinant scFv antibody expression. Lane 1: Molecular weight marker; lane 2: concentrated supernatant and periplasmic fractions of isolated scFv; lane 3: Eluted sample from immobilized metal ion affinity chromatography column showing purified scFv. (B) Binding kinetics of scFv to human monomer α-synuclein. Binding of scFv to monomeric α-synuclein was determined by surface plasmon resonance using a BIAcore X biosensor. Six different scFv concentrations (997.5, 665, 498, 332.5, 249.38, and 166.25 nM) at a flow rate of 30 μL/min, were passed over a CM-5 sensor chip to which α-synuclein (20 μg/mL) had been coupled. The association and dissociation constants for the scFv were calculated by fitting the data to a single binding model.

scFv Inhibition of α-Synuclein Aggregation. To determine if purified scFvs could alter α-synuclein aggregation, we co-incubated equimolar concentrations of α-synuclein and scFv and followed the aggregation rate using thioflavin T (ThT) fluorescence staining and aggregate morphology using AFM imaging. ThT is a fluorescent dye that specifically binds to fibrillar structures (*44*). Incubation of 40 μM α-synuclein alone shows a time-dependent increase in fluorescence, as the α-synuclein begins to aggregate (Figure 3A). However, when α-synuclein is incubated with an equimolar concentration of the scFv, there is a substantial decrease in the aggregation rate (Figure 3A,B). Inhibition of α-synuclein aggregation by the scFv is also dose dependent (Table 1). Co-incubation of 40 μM α-synuclein with equimolar concentrations of either a nonspecific control scFv or a nonspecific control protein (phosphorylase B) resulted in rapid precipitation of the protein mixtures precluding determination of aggregation kinetics for these control samples by ThT staining (data not shown).

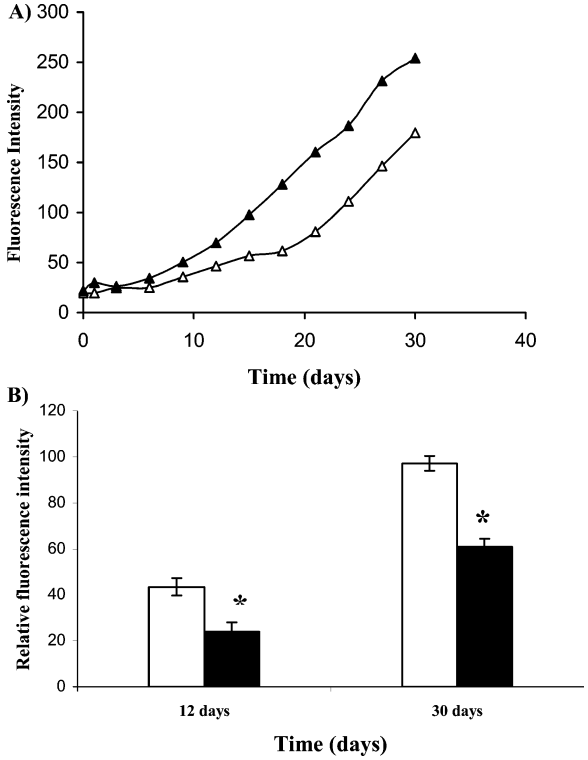

FIGURE 3: Effect of scFvs on the α-synuclein aggregation. The kinetics of α-synuclein fibril formation was monitored by thioflavin T fluorescence in the presence (Δ,■) and absence (▲,□) of equimolar concentrations of ScFv (40 μM). The samples were incubated at 37 °C and 30 μL of samples was added to 2 mL of 5 μM Thio T. Fluorescence intensity was measured at excitation wavelength 450 nm and emission wavelength 482 nm. (A) Data from a single sample showing change in aggregation with time. (B) Data obtained from four independent experiments at 12 and 30 days normalized to 100% for the 30 day sample value without scFv. A p value < 0.05 was considered to be statistically signifficant.

Table 1: Dose Dependence of scFv on α-Synuclein Aggregation[a]

scFv concentration (μM)	% inhibition compared to control
5	2.8
10	6.4
20	20.2
40	32.8

[a] 40 μM of α-synuclein was incubated with different concentrations (5−40 μM) of scFv at 37 °C for 12 days. Data are expressed as percentage inhibition with respect to a control α-synuclein sample without scFv.

Further evidence that the scFv inhibits α-synuclein aggregation is obtained from AFM imaging. After incubation of the sample at 37 °C for 12 days, AFM images indicate the presence of small amorphous aggregates with a root-mean-square (rms) radius of 1.822 nm in the sample without scFv (Figure 4A), while the sample incubated with equimolar concentration of scFv (40 μM) (Figure 4C) had substantially fewer amorphous aggregates of smaller size (rms = 0.823 nm). After 30 days, the α-synuclein sample incubated without scFv shows extensive protofibril or filament formation having diameters of 1.97 ± 0.36 nm (Figure 4B), whereas the sample incubated with scFv did not show any formation of protofibrils or filaments, and only a moderate increase in the presence of amorphous aggregates (rms = 1.021 nm) compared to the 12-day sample (Figure 4C,D). In addition, a height

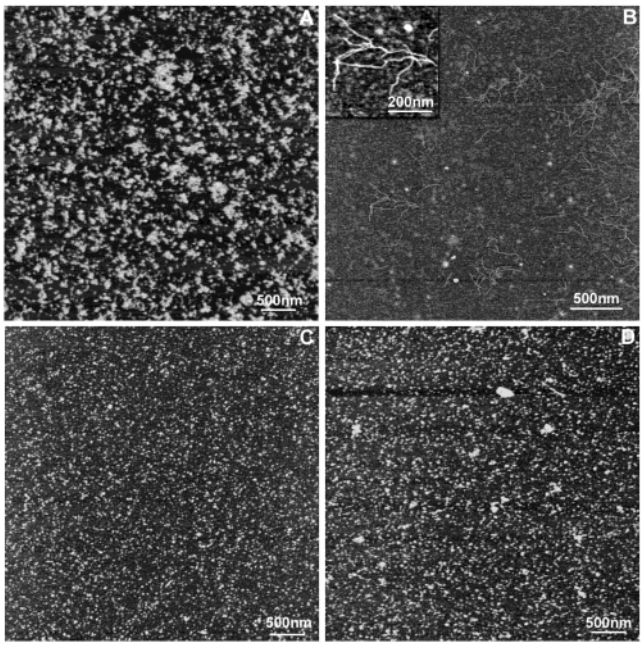

FIGURE 4: Imaging of scFv inhibition of α-synuclein aggregation. AFM analysis of α-synuclein aggregates in the presence and absence of scFv: (A) α-synuclein (40 μM), 12 days; (B) α-synuclein (40 μM), 30 days; (C) α-synuclein/scFv (40/40 μM), 12 days; (D) α-synuclein/scFv (40/40 μM), 30 days. The scale bars represent 500 nm; the height scales are for (A) 15, (B) 4, (C) 8, and (D) 8 nm.

Table 2: Aggregate Height Distribution[a]

molecule height (nm)	<1	1−2	2−3	3−4	4−5	5−6	>6
α-synuclein 12 days (%)	55.90	13.10	12.10	8.20	5.80	2.90	2.00
α-synuclein + scFv 12 days (%)	86.30	7.70	3.90	0.50	0.50	0.10	0.00
α-synuclein + scFv 30 days (%)	80.30	12.50	4.40	0.60	0.60	0.20	0.30

[a] α-Synuclein (40 μM) with and without added scFv (40 μM) was incubated at 37 °C for 12 and 30 days. Data represents the height distribution analysis of the aggregates observed in the AFM images.

distribution analysis of the aggregates in the AFM images showed substantial differences in the aggregate sizes obtained when α-synuclein is incubated with scFv as compared to the control sample without scFv. In the α-synuclein control sample, after 12 days 44.1% of the aggregate particles had heights greater than 1 nm, ranging from 1 to 2 nm to greater than 6 nm (Table 2). In contrast, in the α-synuclein sample co-incubated with scFv, after 12 days, the height distribution of the aggregates showed much smaller particles, with 86.3% having heights less than 1 nm (Table 2). There is only a slight increase in the aggregate height distribution in the scFv sample from day 12 to day 30 (Table 2), whereas the control sample shows substantial formation of protofibrils (Figure 4B).

DISCUSSION

Aberrant processing and aggregation of proteins is a pathological aspect of numerous neurodegenerative diseases including not only Parkinson's and the related synucleinopathies, but also Alzheimer's, Huntington's, and prion

diseases (*45*−*48*). Recently, neuropathologic and genetics studies as well as the development of transgenic animal models have provided strong evidence for the involvement of misfolding and aggregation of α-synuclein in the progression of PD (*13*, *14*, *21*) and other related diseases (*5*, *6*, *8*, *9*). While the exact role of α-synuclein misfolding in PD is still unclear, a number of different α-synuclein aggregate morphologies and conditions that favor them have been identified (*18*, *24*, *49*−*51*). Different aggregate morphologies of α-synuclein have been shown to be more neurotoxic than the monomeric form (*52*). Recently, it was shown that antibodies that bind a toxic oligomeric conformation of *β*-amyloid implicated in Alzheimer's disease, also bind oligomeric structures of α-synuclein as well as other oligomeric proteins involved in Huntington's, type II diabetes, and prion-related diseases (*53*). Therefore, there is growing evidence that controlling folding of the implicated proteins in each of these diseases can have therapeutic value.

Several different strategies have been attempted to control aggregation of α-synuclein. For example, the conformation of α-synuclein can be modulated by metals, with iron promoting and magnesium inhibiting aggregation (*54*, *55*), providing a potential explanation for previous studies that indicated metals play an important role in the pathophysiology of neurodegenerative disorders including PD (*56*−*60*). Other factors such as lipid binding, phosphorylation, and addition of *β*-synuclein have all been shown to change the conformation of α-synuclein, resulting in either inhibition or promotion of α-synuclein aggregation (*61*−*65*). Inhibition of fibril formation was reported by co-incubating human and mouse α-synuclein (*26*). The C-terminal domain of α-synuclein has also been shown to modulate α-synuclein aggregation (*22*, *66*, *67*). Here we demonstrate that scFv fragments can be used to alter α-synuclein folding and aggregation and therefore may have therapeutic application for controlling the progression of PD and other related synucleinopathies. Previously, an scFv targeting a sequence N-terminal to the polyQ region of the huntingtin protein was expressed intracellularly and shown to inhibit aggregation of mutant huntingtin-exon 1 in several cell lines, demonstrating the potential of intrabodies to alter protein aggregation (*33*). Furthermore, this intrabody also provides functional protection against huntingtin-specific toxicity when transfected into organotypic slice cultures of the mouse brain (*31*), and a separate intrabody targeting a sequence C-terminal to the polyQ also inhibited aggregation and improved survival in nonneuronal cell lines (*32*).

The data presented in this study provide evidence that scFv's isolated from a human naïve phage display antibody library (*34*) can control α-synuclein folding. After five rounds of panning, we selected the best binding full-length scFv as determined by ELISA for further functional studies. Kinetic analysis indicated that scFv bound monomeric α-synuclein with relatively high affinity ($K_D = 2.5 \times 10^{-8}$ M). The scFv inhibits the α-synuclein aggregation rate by around 30%, increases the lag time before aggregation starts (Table 1 and Figure 3), and alters the morphology of the aggregates. AFM images show substantial formation of protofibrils after 30 days in the α-synuclein control sample, while the sample incubated with scFv shows formation of only small amorphous aggregates (Figure 4, Table 2). While other studies report extensive formation of fibrillar aggregates after 30 days (*23*−*25*, *49*), we were interested in studying inhibition rather than formation of aggregates, so in contrast to the previous studies, we used a lower substrate concentration (40 μM) and did not utilize stirring, since both high concentrations and stirring favor rapid formation of α-synuclein fibrils (*19*, *25*, *68*). The lower substrate concentration utilized in the present study is also in the range of the reported concentration of α-synuclein found in the cytoplasm of neurons, 30−60 μM (*69*). The protofibrils formed in our α-synuclein control samples are smaller (1.97 ± 0.36 nm) than the size of protofibrils previously reported (6−8 nm (*52*, *70*) or 4.0 nm (*51*)), most likely attributable to different incubation and imaging conditions.

Protein aggregation can be controlled through different mechanisms. Aggregation can be inhibited either by blocking the nucleation sites that initiate formation of the aggregates, or by preventing the protein from adopting the necessary 3D conformation leading to aggregation. To help identify which region of α-synuclein our scFv was binding to, we utilized peptides from six different regions of α-synuclein to map scFv binding. On the basis of ELISA analysis, the scFv binds peptides 2 and 6 corresponding respectively to residues 27−37 and 101−111 of α-synuclein (Figure 1B). This binding cross-reactivity may reflect binding of the scFv to a six-amino acid sequence (-GKxxEG-) present in both peptides 2 and 6, although the peptide 6 sequence appears to be favored. Since the scFv isolated against monomeric protein also showed strong binding to fibrillar samples of α-synuclein, either the P2 and/or P6 regions of α-synuclein are exposed in the aggregated fibrillar morphology of the protein, or the scFv also recognizes a separate epitope in the aggregated morphology of the protein.

In summary, we show that high-affinity scFv antibody fragments isolated against monomeric α-synuclein can be obtained from a naïve phage display human antibody library, and that these scFv fragments can be used to control α-synuclein aggregation. Other strategies has been used to control α-synuclein aggregation in vivo and in vitro such as *β*-synuclein, magnesium, and the C-terminal truncated forms of human α-synuclein (*55*, *65*−*67*, *71*). The advantage of the human recombinant antibody fragments isolated here over these other methods is that the scFv can be targeted specifically to α-synuclein or even epitopes or morphologies of α-synuclein decreasing any potential negative side effects. Furthermore, scFv fragments can be expressed intracellularly, (called intrabodies) for potential in vivo therapeutic applications (*30*). An scFv against exon-1 of Huntingtin protein that inhibited intracellular aggregation in an overexpression system also showed functional protection when cotransfected into organotypic brain slice cultures brain (*31*). Therefore, the scFv isolated here along with other scFv's isolated against other epitopes of α-synuclein can have potential therapeutic applications when expressed as intrabodies in dopaminergic nerve cells for controlling the pathology of PD.

REFERENCES

1. Schapira, A. H. (1997) Pathogenesis of Parkinson's disease. *Baillieres Clin. Neurol. 6*, 15−36.
2. Spillantini, M. G., Schmidt, M. L., Lee, V. M., Trojanowski, J. Q., Jakes, R., and Goedert, M. (1997) Alpha-synuclein in Lewy bodies. *Nature 388*, 839−840.
3. Spillantini, M. G., Crowther, R. A., Jakes, R., Hasegawa, M., and Goedert, M. (1998) alpha-Synuclein in filamentous inclusions of

Lewy bodies from Parkinson's disease and dementia with lewy bodies. *Proc. Natl. Acad. Sci. U.S.A. 95*, 6469−6473.
4. Baba, M., Nakajo, S., Tu, P. H., Tomita, T., Nakaya, K., Lee, V. M., Trojanowski, J. Q., and Iwatsubo, T. (1998) Aggregation of alpha-synuclein in Lewy bodies of sporadic Parkinson's disease and dementia with Lewy bodies. *Am. J. Pathol. 152*, 879−884.
5. Wakabayashi, K., Yoshimoto, M., Tsuji, S., and Takahashi, H. (1998) Alpha-synuclein immunoreactivity in glial cytoplasmic inclusions in multiple system atrophy. *Neurosci. Lett. 249*, 180−182.
6. Wakabayashi, K., Hayashi, S., Ishikawa, A., Hayashi, T., Okuizumi, K., Tanaka, H., Tsuji, S., and Takahashi, H. (1998) Autosomal dominant diffuse Lewy body disease. *Acta Neuropathol. (Berlin) 96*, 207−210.
7. Wakabayashi, K., Hayashi, S., Kakita, A., Yamada, M., Toyoshima, Y., Yoshimoto, M., and Takahashi, H. (1998) Accumulation of alpha-synuclein/NACP is a cytopathological feature common to Lewy body disease and multiple system atrophy. *Acta Neuropathol. (Berlin) 96*, 445−452.
8. Tu, P. H., Galvin, J. E., Baba, M., Giasson, B., Tomita, T., Leight, S., Nakajo, S., Iwatsubo, T., Trojanowski, J. Q., and Lee, V. M. (1998) Glial cytoplasmic inclusions in white matter oligodendrocytes of multiple system atrophy brains contain insoluble alpha-synuclein. *Ann. Neurol. 44*, 415−422.
9. Dickson, D. W., Lin, W., Liu, W. K., and Yen, S. H. (1999) Multiple system atrophy: a sporadic synucleinopathy. *Brain Pathol. 9*, 721−732.
10. Kruger, R., Kuhn, W., Muller, T., Woitalla, D., Graeber, M., Kosel, S., Przuntek, H., Epplen, J. T., Schols, L., and Riess, O. (1998) Ala30Pro mutation in the gene encoding alpha-synuclein in Parkinson's disease. *Nat. Genet. 18*, 106−108.
11. Polymeropoulos, M. H., Lavedan, C., Leroy, E., Ide, S. E., Dehejia, A., Dutra, A., Pike, B., Root, H., Rubenstein, J., Boyer, R., Stenroos, E. S., Chandrasekharappa, S., Athanassiadou, A., Papapetropoulos, T., Johnson, W. G., Lazzarini, A. M., Duvoisin, R. C., Di Iorio, G., Golbe, L. I., and Nussbaum, R. L. (1997) Mutation in the alpha-synuclein gene identified in families with Parkinson's disease. *Science 276*, 2045−2047.
12. Singleton, A. B., Farrer, M., Johnson, J., Singleton, A., Hague, S., Kachergus, J., Hulihan, M., Peuralinna, T., Dutra, A., Nussbaum, R., Lincoln, S., Crawley, A., Hanson, M., Maraganore, D., Adler, C., Cookson, M. R., Muenter, M., Baptista, M., Miller, D., Blancato, J., Hardy, J., and Gwinn-Hardy, K. (2003) alpha-Synuclein locus triplication causes Parkinson's disease. *Science 302*, 841.
13. Feany, M. B., and Bender, W. W. (2000) A Drosophila model of Parkinson's disease. *Nature 404*, 394−398.
14. Masliah, E., Rockenstein, E., Veinbergs, I., Mallory, M., Hashimoto, M., Takeda, A., Sagara, Y., Sisk, A., and Mucke, L. (2000) Dopaminergic loss and inclusion body formation in alpha-synuclein mice: implications for neurodegenerative disorders. *Science 287*, 1265−1269.
15. Giasson, B. I., Duda, J. E., Quinn, S. M., Zhang, B., Trojanowski, J. Q., and Lee, V. M. (2002) Neuronal alpha-synucleinopathy with severe movement disorder in mice expressing A53T human alpha-synuclein. *Neuron 34*, 521−533.
16. Davidson, W. S., Jonas, A., Clayton, D. F., and George, J. M. (1998) Stabilization of alpha-synuclein secondary structure upon binding to synthetic membranes. *J. Biol. Chem. 273*, 9443−9449.
17. Giasson, B. I., Murray, I. V., Trojanowski, J. Q., and Lee, V. M. (2001) A hydrophobic stretch of 12 amino acid residues in the middle of alpha- synuclein is essential for filament assembly. *J. Biol. Chem. 276*, 2380−2386.
18. Conway, K. A., Harper, J. D., and Lansbury, P. T., Jr. (2000) Fibrils formed in vitro from alpha-synuclein and two mutant forms linked to Parkinson's disease are typical amyloid. *Biochemistry 39*, 2552−2563.
19. Conway, K. A., Harper, J. D., and Lansbury, P. T. (1998) Accelerated in vitro fibril formation by a mutant alpha-synuclein linked to early-onset Parkinson disease. *Nat. Med. 4*, 1318−1320.
20. Giasson, B. I., Uryu, K., Trojanowski, J. Q., and Lee, V. M. (1999) Mutant and wild-type human alpha-synucleins assemble into elongated filaments with distinct morphologies in vitro. *J. Biol. Chem. 274*, 7619−7622.
21. Narhi, L., Wood, S. J., Steavenson, S., Jiang, Y., Wu, G. M., Anafi, D., Kaufman, S. A., Martin, F., Sitney, K., Denis, P., Louis, J. C., Wypych, J., Biere, A. L., and Citron, M. (1999) Both familial Parkinson's disease mutations accelerate alpha-synuclein aggregation [published erratum appears in *J. Biol. Chem.* 1999, *274*, 13728]. *J. Biol. Chem. 274*, 9843−9846.
22. Serpell, L. C., Berriman, J., Jakes, R., Goedert, M., and Crowther, R. A. (2000) Fiber diffraction of synthetic alpha-synuclein filaments shows amyloid-like cross-beta conformation. *Proc. Natl. Acad. Sci. U.S.A. 97*, 4897−4902.
23. Uversky, V. N., Gillespie, J. R., and Fink, A. L. (2000) Why are "natively unfolded" proteins unstructured under physiologic conditions? *Proteins 41*, 415−427.
24. Uversky, V. N., Li, J., and Fink, A. L. (2001) Metal-triggered structural transformations, aggregation and fibrillation of human alpha-synuclein. A possible molecular link between parkinson's disease and heavy metal exposure. *J. Biol. Chem. 276*, 44284−44296.
25. Hoyer, W., Antony, T., Cherny, D., Heim, G., Jovin, T. M., and Subramaniam, V. (2002) Dependence of alpha-synuclein aggregate morphology on solution conditions. *J. Mol. Biol. 322*, 383−393.
26. Rochet, J. C., Conway, K. A., and Lansbury, P. T., Jr. (2000) Inhibition of fibrillization and accumulation of prefibrillar oligomers in mixtures of human and mouse alpha-synuclein. *Biochemistry 39*, 10619−10626.
27. Li, J., Uversky, V. N., and Fink, A. L. (2001) Effect of familial Parkinson's disease point mutations A30P and A53T on the structural properties, aggregation, and fibrillation of human alpha-synuclein. *Biochemistry 40*, 11604−11613.
28. Li, J., Uversky, V. N., and Fink, A. L. (2002) Conformational behavior of human alpha-synuclein is modulated by familial Parkinson's disease point mutations A30P and A53T. *Neurotoxicology 23*, 553−567.
29. Zhou, W., Hurlbert, M. S., Schaack, J., Prasad, K. N., and Freed, C. R. (2000) Overexpression of human alpha-synuclein causes dopamine neuron death in rat primary culture and immortalized mesencephalon-derived cells. *Brain Res. 866*, 33−43.
30. Marasco, W. A., Haseltine, W. A., and Chen, S. Y. (1993) Design, intracellular expression, and activity of a human anti-human immunodeficiency virus type 1 gp120 single-chain antibody. *Proc. Natl. Acad. Sci. U.S.A. 90*, 7889−7893.
31. Messer, A., and Murphy, R. (2003) A single-chain Fv intrabody provides functional protection against the effects of mutant protein in an organotypic slice culture model of Huntington's Disease. *Mol. Brain Res.*, in press.
32. Khoshnan, A., Ko, J., and Patterson, P. H. (2002) Effects of intracellular expression of anti-huntingtin antibodies of various specificities on mutant huntingtin aggregation and toxicity. *Proc. Natl. Acad. Sci. U.S.A. 99*, 1002−1007.
33. Lecerf, J. M., Shirley, T. L., Zhu, Q., Kazantsev, A., Amersdorfer, P., Housman, D. E., Messer, A., and Huston, J. S. (2001) Human single-chain Fv intrabodies counteract in situ huntingtin aggregation in cellular models of Huntington's disease. *Proc. Natl. Acad. Sci. U.S.A. 98*, 4764−4769.
34. Griffiths, A. D., Williams, S. C., Hartley, O., Tomlinson, I. M., Waterhouse, P., Crosby, W. L., Kontermann, E., Jones, P. T., Low, N. M., Allison, T. J., Prospero, T. D., Hoogenboom, H. R., Nissim, A., Cox, J. P. L., Harrison, J. L., Zaccolo, M., Gherardi, E., and Winter, G. (1994) Isolation of high affinty human antibodies directly from large synthetic repertoires. *EMBO J. 13*, 3245−3260.
35. Marks, J. D., Hoogenboom, H. R., Bonnert, T. P., McCafferty, J., Griffiths, A. D., and Winter, G. (1991) By-passing Immunization Human Antibodies from V-gene Libraries Displayed on Phage. *J. Mol. Biol. 222*, 581−597.
36. Carter, P., Bedouelle, H., and Winter, G. (1985) Improved oligonucleotide site-directed mutagenesis using M13 vectors. *Nucleic Acids Res. 13*, 4431−4443.
37. Tomlinson, I., and Holliger, P. (2000) Methods for generating multivalent and bispecific antibody fragments. *Methods Enzymol. 326*, 461−479.
38. Hochuli, E. (1988) Large-scale chromatography of recombinant proteins. *J. Chromatogr. 444*, 293−302.
39. de Bruin, R., Spelt, K., Mol, J., Koes, R., and Quattrocchio, F. (1999) Selection of high-affinity phage antibodies from phage display libraries. *Nat. Biotechnol. 17*, 397−399.
40. Hoogenboom, H. R., and Winter, G. (1992) By-passing Immunisation Human Antibodies from Synthetic Repertoires of Germline VH Gene Segments Rearranged in Vitro. *J. Mol. Biol. 227*, 381−388.
41. Shlyakhtenko, L. S., Potaman, V. N., Sinden, R. R., Gall, A. A., and Lyubchenko, Y. L. (2000) Structure and dynamics of three-

way DNA junctions: atomic force microscopy studies. *Nucleic Acids Res. 28*, 3472−3477.
42. Shlyakhtenko, L. S., Gall, A. A., Filonov, A., Cerovac, Z., Lushnikov, A., and Lyubchenko, Y. L. (2003) Silatrane-based surface chemistry for immobilization of DNA, protein-DNA complexes and other biological materials. *Ultramicroscopy 97*, 279−287.
43. Bustamante, C., Vesenka, J., Tang, C. L., Rees, W., Guthold, M., and Keller, R. (1992) Circular DNA molecules imaged in air by scanning force microscopy. *Biochemistry 31*, 22−26.
44. LeVine III, H. (1993) Thiflavine T interaction with synthetic Alzheimer's disease β-amyloid peptides: Detection of amyloid aggregation in solution. *Protein Sci. 2*, 404−410.
45. Gutekunst, C. A., Li, S. H., Yi, H., Mulroy, J. S., Kuemmerle, S., Jones, R., Rye, D., Ferrante, R. J., Hersch, S. M., and Li, X. J. (1999) Nuclear and neuropil aggregates in Huntington's disease: relationship to neuropathology. *J. Neurosci. 19*, 2522−25234.
46. DiFiglia, M., Sapp, E., Chase, K. O., Davies, S. W., Bates, G. P., Vonsattel, J. P., and Aronin, N. (1997) Aggregation of huntingtin in neuronal intranuclear inclusions and dystrophic neurites in brain. *Science 277*, 1990−1993.
47. Duda, J. E., Lee, V. M., and Trojanowski, J. Q. (2000) Neuropathology of synuclein aggregates. *J. Neurosci. Res. 61*, 121−127.
48. Bolton, D. C., McKinley, M. P., and Prusiner, S. B. (1982) Identification of a protein that purifies with the scrapie prion. *Science 218*, 1309−1311.
49. Uversky, V. N., Li, J., and Fink, A. L. (2001) Evidence for a partially folded intermediate in alpha-synuclein fibril formation. *J. Biol. Chem. 276*, 10737−10744.
50. Lashuel, H., Petre, B., Wall, J., Simon, M., Nowak, R., Walz, T., and Lansbury, P. (2002) alpha-Synuclein, Especially the Parkinson's Disease-associated Mutants, Forms Pore-like Annular and Tubular Protofibrils. *J. Mol. Biol. 322*, 1089.
51. Conway, K. A., Lee, S. J., Rochet, J. C., Ding, T. T., Williamson, R. E., and Lansbury, P. T., Jr. (2000) Acceleration of oligomerization, not fibrillization, is a shared property of both alpha-synuclein mutations linked to early-onset Parkinson's disease: implications for pathogenesis and therapy. *Proc. Natl. Acad. Sci. U.S.A. 97*, 571−576.
52. El-Agnaf, O. M., Jakes, R., Curran, M. D., Middleton, D., Ingenito, R., Bianchi, E., Pessi, A., Neill, D., and Wallace, A. (1998) Aggregates from mutant and wild-type alpha-synuclein proteins and NAC peptide induce apoptotic cell death in human neuroblastoma cells by formation of beta-sheet and amyloid-like filaments. *FEBS Lett. 440*, 71−75.
53. Kayed, R., Head, E., Thompson, J. L., McIntire, T. M., Milton, S. C., Cotman, C. W., and Glabe, C. G. (2003) Common structure of soluble amyloid oligomers implies common mechanism of pathogenesis. *Science 300*, 486−489.
54. Hashimoto, M., Hsu, L. J., Xia, Y., Takeda, A., Sisk, A., Sundsmo, M., and Masliah, E. (1999) Oxidative stress induces amyloid-like aggregate formation of NACP/alpha-synuclein in vitro. *Neuroreport 10*, 717−721.
55. Golts, N., Snyder, H., Frasier, M., Theisler, C., Choi, P., and Wolozin, B. (2002) Magnesium inhibits spontaneous and iron-induced aggregation of alpha-synuclein. *J. Biol. Chem. 277*, 16116−16123.
56. Atwood, C. S., Moir, R. D., Huang, X., Scarpa, R. C., Bacarra, N. M., Romano, D. M., Hartshorn, M. A., Tanzi, R. E., and Bush, A. I. (1998) Dramatic aggregation of Alzheimer abeta by Cu(II) is induced by conditions representing physiological acidosis. *J. Biol. Chem. 273*, 12817−12826.
57. Bush, A. I., Pettingell, W. H., Multhaup, G., d Paradis, M., Vonsattel, J. P., Gusella, J. F., Beyreuther, K., Masters, C. L., and Tanzi, R. E. (1994) Rapid induction of Alzheimer A beta amyloid formation by zinc. *Science 265*, 1464−1467.
58. Brown, D. R., Qin, K., Herms, J. W., Madlung, A., Manson, J., Strome, R., Fraser, P. E., Kruck, T., von Bohlen, A., Schulz-Schaeffer, W., Giese, A., Westaway, D., and Kretzschmar, H. (1997) The cellular prion protein binds copper in vivo. *Nature* 390, 684−687.
59. Gorell, J. M., Johnson, C. C., Rybicki, B. A., Peterson, E. L., Kortsha, G. X., Brown, G. G., and Richardson, R. J. (1999) Occupational exposure to manganese, copper, lead, iron, mercury and zinc and the risk of Parkinson's disease. *Neurotoxicology 20*, 239−247.
60. Duda, J. E., Giasson, B. I., Chen, Q., Gur, T. L., Hurtig, H. I., Stern, M. B., Gollomp, S. M., Ischiropoulos, H., Lee, V. M., and Trojanowski, J. Q. (2000) Widespread nitration of pathological inclusions in neurodegenerative synucleinopathies. Am. J. Pathol. *157*, 1439−14345.
61. Jo, E., McLaurin, J., Yip, C. M., St George-Hyslop, P., and Fraser, P. E. (2000) alpha-Synuclein membrane interactions and lipid specificity. *J. Biol. Chem. 275*, 34328−34334.
62. Perrin, R. J., Woods, W. S., Clayton, D. F., and George, J. M. (2000) Interaction of human alpha-Synuclein and Parkinson's disease variants with phospholipids. Structural analysis using site-directed mutagenesis. *J. Biol. Chem. 275*, 34393−34398.
63. Fujiwara, H., Hasegawa, M., Dohmae, N., Kawashima, A., Masliah, E., Goldberg, M. S., Shen, J., Takio, K., and Iwatsubo, T. (2002) alpha-Synuclein is phosphorylated in synucleinopathy lesions. *Nat. Cell Biol. 4*, 160−164.
64. Uversky, V. N., Yamin, G., Souillac, P. O., Goers, J., Glaser, C. B., and Fink, A. L. (2002) Methionine oxidation inhibits fibrillation of human alpha-synuclein in vitro. *FEBS Lett. 517*, 239−244.
65. Hashimoto, M., Rockenstein, E., Mante, M., Mallory, M., and Masliah, E. (2001) beta-Synuclein inhibits alpha-synuclein aggregation: a possible role as an anti-parkinsonian factor. *Neuron 32*, 213−223.
66. Murray, I. V., Giasson, B. I., Quinn, S. M., Koppaka, V., Axelsen, P. H., Ischiropoulos, H., Trojanowski, J. Q., and Lee, V. M. (2003) Role of alpha-synuclein carboxy-terminus on fibril formation in vitro. *Biochemistry 42*, 8530−85340.
67. Crowther, R. A., Jakes, R., Spillantini, M. G., and Goedert, M. (1998) Synthetic filaments assembled from C-terminally truncated alpha-synuclein. *FEBS Lett. 436*, 309−312.
68. Ding, T. T., Lee, S. J., Rochet, J. C., and Lansbury, P. T., Jr. (2002) Annular alpha-synuclein protofibrils are produced when spherical protofibrils are incubated in solution or bound to brain-derived membranes. *Biochemistry 41*, 10209−10217.
69. Iwai, A., Masliah, E., Yoshimoto, M., Ge, N., Flanagan, L., de Silva, H. A., Kittel, A., and Saitoh, T. (1995) The precursor protein of non-A beta component of Alzheimer's disease amyloid is a presynaptic protein of the central nervous system. *Neuron 14*, 467−475.
70. El-Agnaf, O. M., and Irvine, G. B. (2000) Review: formation and properties of amyloid-like fibrils derived from alpha-synuclein and related proteins. *J. Struct. Biol. 130*, 300−309.
71. Park, J. Y., and Lansbury, P. T., Jr. (2003) Beta-synuclein inhibits formation of alpha-synuclein protofibrils: a possible therapeutic strategy against Parkinson's disease. *Biochemistry 42*, 3696−3700.

BI036281F